

# Verification for Protection Design of Single Event Lockup with Pulsed Laser

An Heng<sup>1</sup>, Zhang Huaiqing<sup>1\*</sup>, Li Detian<sup>2</sup>, Zhang Chengguang<sup>2</sup>, Yang Shengsheng<sup>2</sup>

## Affiliations:

1. Chongqing University, School of Electrical Engineering, Chongqing 400044, China
2. Lanzhou Institute of Physics, Lanzhou 730000, China

**Abstract:** Pulsed laser testing is a simple, cost-effective, safe, and radiation-free method, offering flexible scheduling, adjustable energy levels, non-destructive testing, and easy operation. It has broad application prospects in simulating single event effects (SEE) in space and has become a mainstream method used domestically and internationally in the past decade, besides the heavy ion accelerator test method. With its ability to accurately target sensitive areas, pulsed laser testing has evolved into a valuable complement to heavy ion experiments, widely used in the performance evaluation of single event effect hardening designs of electronic devices. This paper investigates the single event lockup in image sensors and evaluates the effectiveness of protection strategies using pulsed laser experiments. The research focuses on CMOS APS image sensors, using a focused pulsed laser beam to simulate single event effects. By adjusting the laser's energy and irradiation position, we simulate varying energies and incident angles of SEE, observing the sensor's response. The study provides a detailed analysis of device lockup behavior and evaluates the actual effectiveness of protection methods. The

results show that pulsed laser testing offers an effective means to assess the protection strategies against SEE lockup in image sensors. Through comparative experiments, the advantages and disadvantages of the protection strategies in resisting the single event lockup can be clearly seen, thus providing insights for improved designs in practical space applications.

**Keywords:** Single Event Effects (SEEs), Single Event Lockup, Protection Design, Pulsed Laser, Effectiveness Verification

## 1. Introduction

Single Event Effects (SEEs) are radiation-induced phenomena caused by the interaction of high-energy particles with microelectronic devices. For example, electronic devices in satellites being affected by single event effects during on-orbit operation and in harsh environments like artificial radiation, affecting device functionality. With the rapid advancement of space technology, image sensors are increasingly used in space exploration and remote sensing. Understanding and mitigating SEEs in image sensors has become increasingly important with the widespread use of these devices in space application.

Research on SEEs and their protection strategies in image sensors has been active in recent years. In China, Several institutions, including Chongqing University, Lanzhou Institute of Physics, and Qian Xuesen Laboratory of Space Technology, have conducted significant work in this field. Their work highlights the effectiveness of pulsed laser testing in studying SEL and providing insights for improved designs [1]. Globally, SEE research has been an active area of investigation for decades, with various approaches employed to simulate and mitigate these effects. Heavy ion accelerators have traditionally been the primary tool for SEE testing; however, pulsed laser testing has emerged as a simple, cost-effective, and safe alternative. Researchers worldwide have demonstrated the potential of pulsed laser experiments in evaluating SEE-hardened designs for electronic devices [2-4]. In particular, the use of two-photon absorption laser testing has enabled more accurate simulation of SEEs in semiconductor devices. Studies have shown that this technique can effectively induce SEL in SRAM cells, providing valuable insights into the sensitive depth and failure mechanisms of these devices.

However, in the space environment, image sensors are susceptible to the effects of high-energy particles, leading to SEEs, which can cause malfunctions or reduced performance. Among the various SEEs, single event lockup (SEL) is particularly critical, as it can cause some circuits in the image sensor to lockup for extended periods,

severely affecting normal operation. Therefore, understanding and developing protection strategies against SEL in image sensors is crucial. Protecting image sensors from SEEs, especially SEL, is crucial for their reliable operation in space environments. Current protection strategies include the use of current-limiting resistors and current-limiting low-dropout regulators. These measures have been shown to be effective in limiting the operating current and preventing circuit lockup due to excessive current flow. However, the optimization of these protection strategies and the development of new materials and structures for enhanced protection remain important areas of ongoing research.

In recent years, pulsed laser testing has become a simple, cost-effective, safe, and non-destructive method for studying SEEs. Alongside heavy ion testing, it has become a mainstream approach for SEE testing globally over the past decade [5-7]. It has the advantage of accurate positioning of sensitive areas and has gradually developed into a beneficial supplement to heavy ion experiments for single event effects, widely used in the performance evaluation of SEE-hardened designs for electronic devices [8-10].

This paper examines the effects of SEL in image sensors using pulsed laser, and analyzes the impact of single event lockup (SEL) on its performance, and verifies the effectiveness of SEL protection strategies through experimental evaluation.

## 2. Principle and Method

SEL occurs when a space radiation particle strikes an MOS device, generating a large current pulse that alters the device's performance. This study uses a focused pulsed laser beam to simulate SEE and conducts experimental research on the SEL effect of CMOS APS image sensors. The experimental setup mainly includes a pulsed laser, an optical system, image sensor samples, and test circuits. By adjusting the energy and irradiation position of the pulsed laser, SEEs with different energy levels are simulated, and the response of the image sensor is observed and recorded. In pulsed laser testing, when a short, intense laser pulse interacts with the silicon semiconductor material of the devices, it initiates a process of photon absorption, which results in the creation of electron-hole pairs. This fundamental process is critical to understanding the effects of SEEs and is governed by the photoelectric effect in semiconductors. If this pulse persists, it can significantly degrade performance or even cause the device to burn out.

The photoelectric effect in silicon can be described by the Einstein equation of photoelectric effect, which relates the energy of the incident photon ( $E_{\text{photon}}$ ) to the energy needed to create an electron-hole pair ( $E_{\text{gap}}$ ) plus the kinetic energy ( $E_k$ ) of the emitted electron:

$$E_{\text{photon}} = E_{\text{gap}} + E_k \quad (1)$$

For silicon at room temperature, the bandgap energy ( $E_{\text{gap}}$ ) is approximately 1.12

eV. The energy of a photon ( $E_{\text{photon}}$ ) is given by the Planck-Einstein relation:

$$E_{\text{photon}} = \frac{h}{\nu} \quad (2)$$

where ( $h$ ) is Planck's constant and ( $\nu$ ) is the frequency of the photon. For laser light with a wavelength of 1064 nm (used in our experiments), the photon energy can be calculated as:

$$E_{\text{photon}} = \frac{hc}{\lambda} \quad (3)$$

Where,  $h=6.626 \times 10^{-34}\text{J}$ ,  $c=2.998 \times 10^8\text{m/s}$ ,  $\lambda=1064 \times 10^{-9}\text{m}$ . So for 1064nm, the  $E_{\text{photon}}$  is approximately 1.85eV.

Since ( $E_{\text{photon}} > E_{\text{gap}}$ ), the photon has sufficient energy to excite an electron from the valence band to the conduction band, leaving behind a positively charged hole. The excess energy above the bandgap is converted into kinetic energy of the electron.

The probability of photon absorption ( $P_{\text{abs}}$ ) in a semiconductor can be approximated using the Beer-Lambert law, which states that the intensity ( $I$ ) of light decreases exponentially with the thickness ( $x$ ) of the material:

$$I(x) = I_0 \cdot e^{-\alpha x} \quad (4)$$

where ( $I_0$ ) is the incident intensity and  $\alpha$  is the absorption coefficient of silicon at the laser wavelength. For silicon at 1064 nm,  $\alpha$  is relatively small, indicating that a substantial fraction of the laser light can penetrate the material before being absorbed.

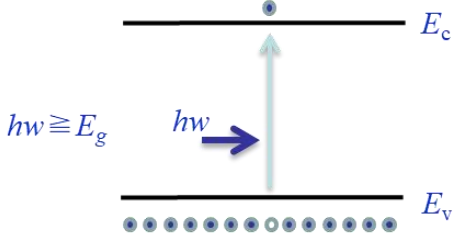
Upon absorption, the electron-hole pairs are generated at a rate proportional to the absorbed photon flux. These charge carriers can then interact with the semiconductor lattice, causing local heating, ionization of neighboring atoms, and potentially leading to SEL in sensitive circuits.

When a short, intense laser pulse interacts with a target, it can lead to a rapid increase in the free electron density, causing the target material to transition from solid to plasma. This transition is critical for various applications, including laser ablation and ion acceleration. The initial stage of this interaction involves photon ionization, where the intense electric field of the laser pulse causes electrons to be liberated from their atomic bonds. As the intensity of the laser pulse increases, more electrons are freed, and the plasma density rises. Once a critical density of free electrons is reached, the plasma becomes highly over-dense, and its dynamics are driven by processes like collisional ionization, plasma expansion, and the formation of a plasma sheath. In the context of SEE, the plasma formed around a particle can lead to the ejection of material through laser ablation. This ablation can result in the formation of nanoparticles or the emission of ions, which can be analyzed for their elemental composition and structural information. Plasma expansion also influences ion acceleration by generating an electric field that drives the process.

In generally, photons with energy greater than semiconductor bandgap will be absorbed directly, creating electron-hole(e-h)

pairs[11]. The relation between photon energy( $E_{\text{photon}}$ ) and light wavelength( $\lambda$ ) is given as equation (3). From this equation, it can be seen that the absorption process is linear when photon energy is more than semiconductor bandgap, that is, a photon can create a pair of electron-hole. This process is called as Single Photon Absorption (SPA), as shown in Fig.1. However, for photon energy less than the semiconductor bandgap, a photon can not create a pair of e-h, so multiphoton may be absorbed [12], as shown in Fig.1.

### Single Photon Absorption (SPA)



### Two Photon Absorption (TPA)

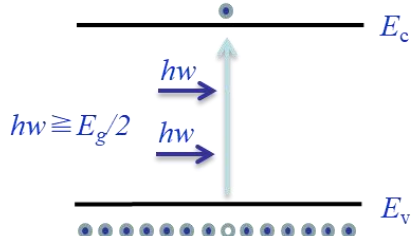


Fig.1 SPA and TPA

In Fig.1,  $hw$  is photon energy,  $E_g$  is energy of semiconductor bandgap( $E_{\text{gap}}$ ).

In our experiments, the focused pulsed laser beam simulates SEEs by precisely depositing energy into the silicon material, triggering the generation of electron-hole pairs and subsequent effects. By adjusting the laser's energy and irradiation position, we simulate varying energies and incident

angles of SEE, observing the sensor's response and evaluating the effectiveness of protection strategies.

### 3. Experimental Methods and Process

#### 3.1 Experimental Devices and Protective Circuit Design

The typical protection strategy for SEL involves adding current-limiting resistors and performing a power-off restart. In this study, current-limiting resistors and current-limiting low-dropout regulators are designed in the circuit, mainly used to limit working current and output current to prevent the occurrence of single event lockup effects.

To verify the effectiveness of the protection strategy, experiments were conducted on image sensors with added current-limiting resistors and low-dropout regulators, inducing SEE through pulsed laser irradiation[13-15]. Inserted in series with the power supply to restrict current Using Low-Dropout Regulator (LDO) , features an enable pin controlled by an FPGA to disconnect power during SEL.Utilizes an embedded ADC (12-bit resolution, 1 MS/s sampling rate) to measure voltage across the shunt resistor.

Preliminary research revealed that the control circuit of the image sensor is particularly sensitive to SEL. Therefore, this design incorporates real-time current monitoring and an overcurrent power-off restart mechanism for protection. The basic principle of this protective strategy is illustrated in Fig.2.

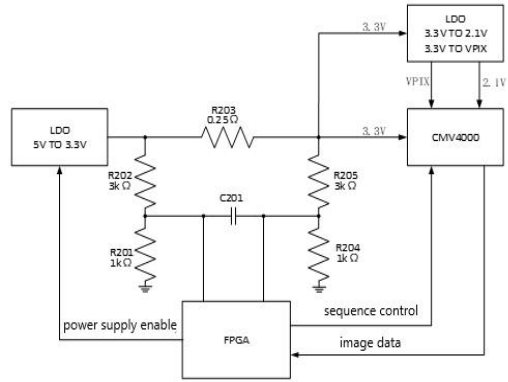


Fig.2 Schematic diagram of single event lockup protection measures

An independent power supply loop is used, with a voltage regulator featuring an enable control pin serving as the sensor's main power supply. The FPGA's built-in AD conversion module is used to monitor the total current of the image sensor in real-time. When the image sensor locks, the supply current will abnormally increase. The FPGA detects when the supply current exceeds a set threshold and maintains it for a specified duration. Then, it controls the power supply enable pin to turn off the output of the total power supply voltage regulator (5V to 3.3V). After the voltage regulator cuts off the image sensor's power supply for 1 second, the FPGA restores power following the correct sequence.

The experiments focused on three key areas: 1) normal working current test of CMOS APS image sensor (CMV4000), 2) current test when single event lockup occurs, and 3) verification of the effectiveness of single event lockup protection. The basic experimental setup is shown in Fig.3.

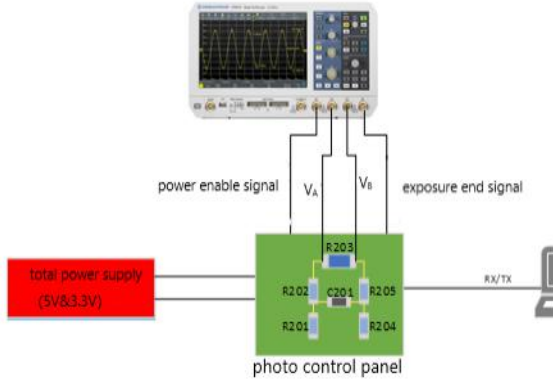


Fig.3 Schematic diagram of the basic connection for experimental testing

In Fig.3, the power enable signal controls the activation and deactivation of the total power supply of the APS image sensor; the exposure end signal is used to mark the end of the APS image sensor's photo exposure, after which data is prepared for output;  $V_A$  is the voltage at the high end of the total power supply shunt resistor of the APS image sensor (the positive end of R203) and  $V_B$  is the voltage at the low end (the negative end of R203).

The voltage difference between  $V_A$  and  $V_B$  directly indicates the working current of the image sensor. By measuring the voltage difference across the shunt resistor, the working current of the image sensor can be monitored in real time.

### 3.2 Pulsed Laser Experiment System

The experimental pulsed laser has a wavelength of 1064 nm, a pulse width of 25ps, a spot diameter of 2 $\mu$ m, a pulse frequency of 10Hz, and a magnification of 20x for the objective lens. The pulsed laser emission, XYZ displacement precision control moving platform control, pulsed laser energy selection, energy testing, focused beam spot testing, and scanning positioning are all computer-controlled [11].

The pulsed SEE experiment system is shown in Fig.4.

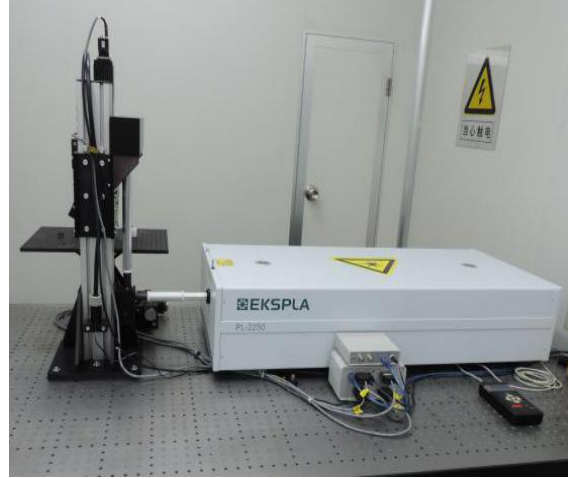


Fig.4 Pulsed laser single event effect experimental equipment

## 4. Experimental Data Analysis

### 4.1 Sensor Normal Working State

The maximum current of the sensor should be during the period when image data is output through LVDS. The experiment measured the total supply current waveform of the APS image sensor by sending a capture command and using the exposure end signal as the trigger condition, as shown in Fig.5. The waveforms from multiple measurements were consistent and repeatable.

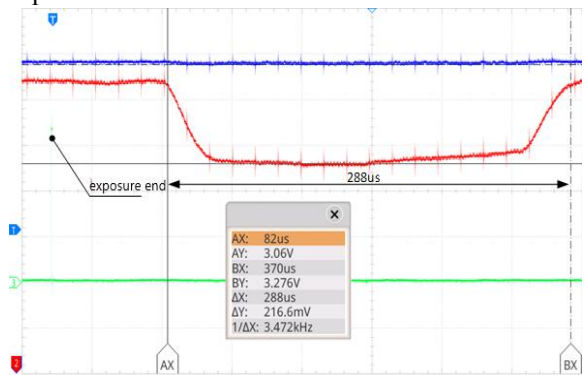


Fig.5 Voltage waveform during image data transfer after photo-taking

Under normal operating conditions, the current waveform of the APS image sensor,

as shown in Fig. 5, illustrates the changes in current during image data transfer. The real-time current monitoring mechanism, as depicted in Fig. 2, ensures that the sensor's current remains within a stable range during normal operation. Calculations from the waveform diagram reveal that during data output, the sensor's operating current significantly increases, attributable to increased activity within the sensor's internal circuits, aligning with the current monitoring and power supply control logic described in Fig. 2.

The following working parameters of the APS sensor in the mini camera can be calculated from the waveform in Fig. 5. The working current during the camera's data output process is  $44\text{mV}/0.253\Omega=174\text{mA}$ . The working current during the data output process is  $216\text{mV}/0.253\Omega=854\text{mA}$ , and the peak current during the data output process lasts about  $288\mu\text{s}$ .

#### 4.2 Single event Lockup Current Test

Pulsed laser SEE experiments were performed on the APS image sensor selected for the mini camera. The experiment used the PL-2250 (EKSPA), and the placement of the image sensor and test circuit is shown in Fig. 6.

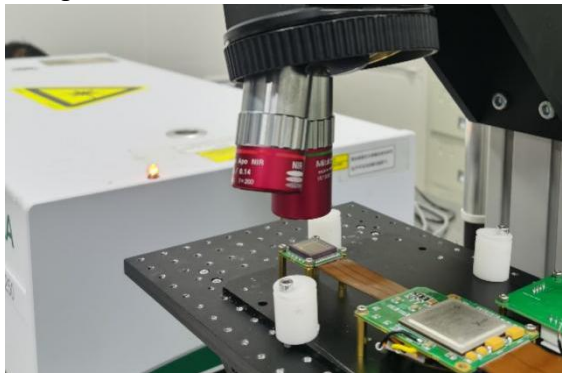


Fig.6 Experimental photo

The test chip remained sealed with its transparent glass protective window. During the experiment, the peripheral control circuit of the image sensor was divided into three areas: A, B, and C, as shown in Fig. 7.

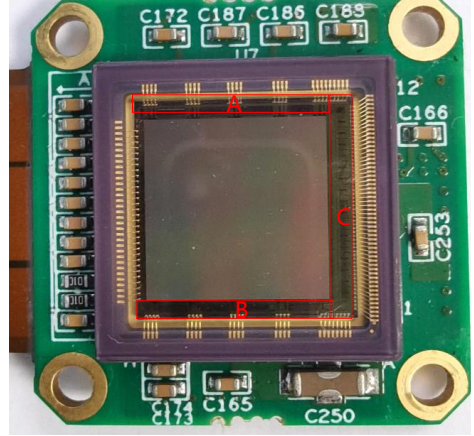


Fig.7 Schematic diagram of scanning partition

During the single event lockup (SEL) testing, by adjusting the pulsed laser energy and scanning the sensitive regions of the image sensor, we successfully induced SEL phenomena. As shown in Fig. 6 and Fig. 7, when the laser energy reached  $7\text{nJ}$  and illuminated a specific location, the sensor's operating current abruptly surged, as depicted in Fig. 8. This phenomenon confirms the occurrence of SEL and demonstrates the response capability of the protection circuit during SEL events.

The test circuit was powered on, and commands were sent through the serial port to verify the device's operational state. The laser energy was adjusted from  $0.1\text{nJ}$  to  $7\text{nJ}$ , scanning the three target areas. The experiment found that when the laser energy of  $7\text{nJ}$  scanned the range (14338, 4206) — (27780, 5649) in area B, there was a phenomenon of a sharp increase in the supply current, which was determined to be

a single event lockup, and the lockup phenomenon could be replicated. After lockup, the total supply current of the APS image sensor increased significantly. At position (15488, 4891), the current and voltage waveforms collected from the shunt resistor terminals and current probes during multiple reproductions of the lockup phenomenon were consistent, as shown in Fig.8. The current increased to about twice the standby working current.

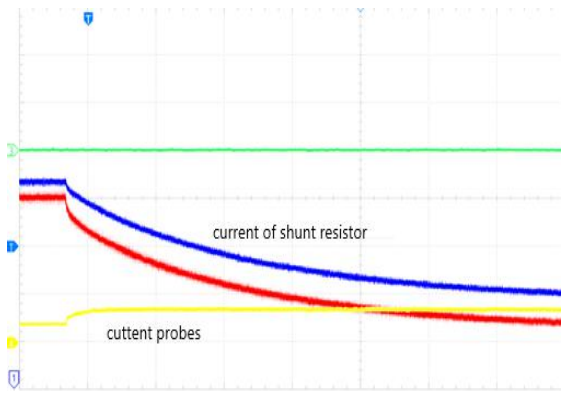


Fig.8 Waveform diagram of the voltage difference across the shunt resistor ends during SEL

#### 4.3 Single event Lockup Protection Verification

During the protection strategy verification phase, repeated triggering of SEL events and observation of the protection circuit's response validated the effectiveness of the protection measures. As depicted in Fig. 9 and Fig. 10, upon SEL occurrence, power is swiftly disconnected, causing the current and voltage waveforms to drop rapidly. Subsequently, after a 1-second delay, power is restored, and the sensor resumes normal operation. This process aligns perfectly with the overcurrent protection and restart mechanism outlined in Fig. 2.

The current protection threshold was set via instructions based on the current measured during lockup. The laser energy of 7nJ was used to repeatedly trigger SEL at the sensitive point (15488, 4891) to verify the effectiveness of the protection measures.

Fig.9 illustrates the complete process of a SEL protection measure with a time scale of 150ms. When the current surpasses the threshold, the power enable signal rises to a high level, turning off the output of the total power LDO chip. After a 1-second interval, the power enable signal outputs a low-level signal, the total power LDO chip output is turned on, and the APS image sensor is powered up again.

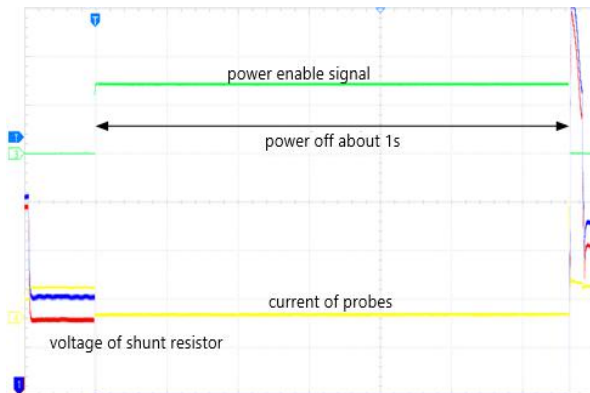


Fig.9 Waveform of the entire process of a single event lockup protection measure

In conjunction with the circuit design in Fig. 2, upon the occurrence of SEL, the abnormal increase in operating current is promptly detected by the FPGA through the AD conversion module, triggering the overcurrent protection mechanism. As illustrated in Fig. 9, when the current exceeds the preset threshold, the FPGA controls the power enable signal to rise to a high level, cutting off the output of the total power LDO chip, thereby achieving a rapid response and suppression of the SEL event.

Once the APS image sensor is powered on, a capture command is sent via the serial port to the test circuit controller to verify whether the sensor is functioning normally. The imaging window of the APS image sensor chip is exposed to light, a photo is taken, and image data are read. Under normal conditions, the data read "0FFF", indicating all pixels are saturated at the maximum level.

A black cover is placed over the APS sensor's imaging window, a photo is taken, and image data are read. As expected, the data shows non-saturated output, which is consistent with the photosensitive characteristics of the chip.

The power-off waveform during SEL (the time scale is 2ms) is shown in Fig.10. When the current exceeds the threshold value, the power enable signal outputs a high level, turning off the output of the total power LDO chip. Voltage and current waveforms drop rapidly. After this waveform collection, the APS image sensor was verified to be functioning normally after a capture command was sent following power restoration.



Fig.10 Waveform of the power supply being turned off during SEL protection

Further analysis reveals that the current-limiting resistors and current-limiting low-dropout linear regulators (LDOs) play pivotal roles in the protection circuit. The current-limiting resistors prevent circuit lockup by restricting the operating current. Meanwhile, the current-limiting LDOs automatically adjust when the output current exceeds the threshold, maintaining the output current within a safe range, effectively preventing the occurrence of SEL.

Figure 11 shows the power supply waveform during a single event lockup, with a time scale of 2ms. After the power supply is turned off for 1s, the power enable signal drops to low level, activating the total power LDO chip output. This results in a current overshoot pulse lasting approximately 1.5ms, followed by a 5ms stabilization in the voltage waveform. After this waveform collection, the APS image sensor was verified to be in a normal working state after being powered on again by sending a photo-taking command.

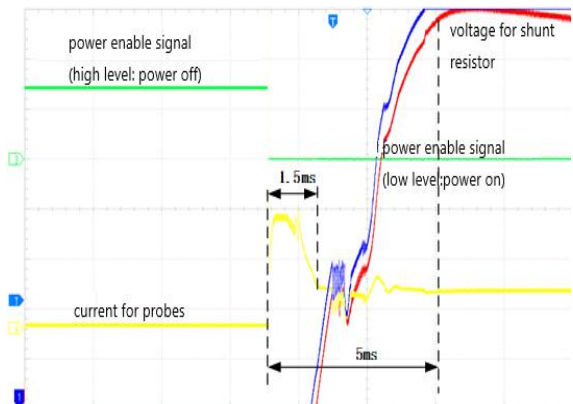


Fig.11 Waveform of the power supply being turned on again during a SEL protection

The experiment demonstrates that a single event lockup occurs when the CMOS APS image sensor is exposed to a pulsed laser.

When the pulsed laser energy reaches a certain threshold, some circuits of the image sensor are locked, leading to abnormally high output signals. Additionally, the results indicate that the image sensor with added current-limiting resistors and current-limiting low-dropout regulators shows better performance in resisting the single event lockup.

Specifically, the current-limiting resistor can effectively restrict the operating current, preventing circuit lockup due to excessive current flow. However, the use of current-limiting resistors is limited to CMOS integrated devices with small dynamic working currents and a large ratio of latch-up current to working current. In contrast, the current-limiting low-dropout regulator offers greater flexibility. It can automatically maintain the output current at the threshold value when the output current exceeds the threshold, thereby effectively preventing the occurrence of single event lockup. However, the threshold value of the current-limiting low-dropout regulator is usually fixed and difficult to perfectly match the lockup current of the protected device, which to some extent affects its protection effect.

By comparing the experimental data before and after implementing the protection strategies, the effectiveness of these strategies in suppressing SEL is evident. With the protection measures in place, the sensor promptly resumes normal operation even under high-energy laser exposure, ensuring system stability and reliability.

In conclusion, the protection strategies designed in this study exhibit superior performance in mitigating SEL events, providing effective protection for image sensors in space applications. Additionally, the experimental results validate the efficacy and reliability of pulsed laser testing in assessing SEE protection strategies.

## 5. Results and Prospects

This paper investigates the single event lockup in image sensors and evaluates protection strategies through pulsed laser experiments. The results confirm that pulsed laser technology is an effective simulation tool for studying single event lockup and can inform practical protection designs. The study shows that current-limiting resistors and current-limiting low-dropout regulators have a certain role in protecting against single event lockup. However, how to further optimize the protection strategy and improve the ability of image sensors to resist single event lockup in the space environment is still a key point for future research. Future research could focus on: (1) further explore new types of protective materials and structures to improve protection effects, (2) study more accurate pulsed laser simulation methods to better simulate actual single events in the space environment[16], (3) strengthen the combination with practical applications, apply research results to the protection design of image sensors against single event effects in actual spacecraft, and improve their reliability and stability in the space environment.

## References

1. Cui Yi-Xin, Ma Ying-Qi, Shangguan Shi-Peng, et al. Research on Single Event Burnout of GaN power devices with femtosecond pulsed laser [J]. *Acta Physica Sinica*, 2022, 71(13):301-310.
2. E. Faraud, V. Pouget, K. Shao, C. Larue, et al., Investigation on the SEL Sensitive Depth of an SRAM Using Linear and Two-Photon Absorption Laser Testing[J]. *IEEE TRANSACTIONS ON NUCLEAR SCIENCE*. 2011, 58(6): 2637-2643.
3. McMorrow.D, Buchner.S, Lotshaw.WT, et al. Demonstration of single-event effects induced by through-wafer two-photon absorption[J]. *IEEE TRANSACTIONS ON NUCLEAR SCIENCE*, 2004, 51(6): 3553-3557.
4. Hales, JM; Roche, NJH; Khachatrian, A; et al. Two-Photon Absorption Induced Single-Event Effects: Correlation Between Experiment and Simulation[J]. *IEEE TRANSACTIONS ON NUCLEAR SCIENCE*, 2015, 62(6): 2867-2873.
5. Faraud, E; Pouget, V; Ecoffet, R; et al. Investigation on the SEL Sensitive Depth of an SRAM Using Linear and Two-Photon Absorption Laser Testing[J]. *IEEE TRANSACTIONS ON NUCLEAR SCIENCE*, 2011, 58 (6):2637-2643.
6. Stephen P. Buchner, Florent Miller, Vincent Pouget, et al., Pulsed-Laser Testing for Single-Event Effects Investigations. *IEEE TRANSACTIONS ON NUCLEAR SCIENCE*. 2013, 60( 3):1852-1875.
7. An Heng, Li Detian, Yang Shengsheng, et al. High-Speed PWM Single Event Transients Pulsed Laser Simulation Test Research[J], *Infrared and Laser Engineering*, 2020, 49(8): 74-80.
8. Joel M. Hales, Ani Khachatrian, Stephen Buchner, et al. A Simplified Approach for Predicting Pulsed-Laser-Induced Carrier Generation in Semiconductors[J]. *IEEE TRANSACTIONS ON NUCLEAR SCIENCE*, 2017, 64(3): 1006-1013.
9. McMorrow, D., Buchner, S., Lotshaw, W. T., et al., Demonstration of single-event effects induced by through wafer two-photon absorption[J], *IEEE Transactions on Nuclear Science*, 2004, 51(6):3553-3557.
10. Hales, J. M., A. Khachatrian, N. J.-H. Roche et al., Simulation of Laser-Based Two-Photon Absorption Induced Charge Carrier Generation in Silicon[J], *IEEE Transactions on Nuclear Science*, 2015, 62(4), 1-8.
11. Zhang Chenguang, An Heng, Wang Yi, et al. Pulsed Laser Simulation of Single event Effects Research[J]. *Nuclear Technology*, 2020, 43 (4):58-63.
12. An Heng, Li Detian, Yang

- Shengsheng, et al. Research Status and Development Trend of Femtosecond Pulsed Laser Single Event Effects Evaluation Technology[J]. Nuclear Technology,2021,44(11): 1-11.
13. Ray Ladbury. Strategies for SEE Hardness Assurance—From Buy-It-And-Fly-It to Bullet Proof[J]. 2017 IEEE Nuclear and Space Radiation Effects Conference(NSREC 2017), New Orleans, LA, July 17-21, 2017.
14. Joel M. Hales, Nicolas J-H. Roche, Ani Khachatrian, et al. Strong Correlation Between Experiment and Simulation for Two-Photon Absorption Induced Carrier Generation[J].IEEE TRANSACTIONS ON NUCLEAR SCIENCE,2017,64(5): 1133-1136.
15. Joel M. Hales , Ani Khachatrian, Stephen Buchner,et al. Experimental Validation of an Equivalent LET Approach for Correlating Heavy-Ion and Laser-Induced Charge Deposition[J].IEEE TRANSACTIONS ON NUCLEAR SCIENCE, 2018,65(8): 1724-1733.
16. Xiaohu Wang, Xuefeng Zheng, Danmei Lin, et al. Study on the single-event burnout mechanism of p-GaN gate AlGaN/GaN HEMTs[J]. Appl. Phys. Lett. 124, 173502 (2024).